Journal of Cancer Research and Clinical Oncology (2019) 145:2433–2444
https://doi.org/10.1007/s00432-019-02995-z

ORIGINAL ARTICLE – CANCER RESEARCH

Stress-triggered YAP1/SOX2 activation transcriptionally reprograms head and neck squamous cell carcinoma for the acquisition of stemness

Hirofumi Omori[1,2] · Kuniaki Sato[1] · Takafumi Nakano[1] · Takahiro Wakasaki[2] · Satoshi Toh[1] · Kenichi Taguchi[3] · Takashi Nakagawa[2] · Muneyuki Masuda[1]

Received: 11 May 2019 / Accepted: 5 August 2019 / Published online: 4 September 2019

Abstract

Purpose The clinical importance of cancer stem cells (CSCs) in head and neck squamous cell carcinoma (HNSCC) is well recognized. However, a reliable method for the detection of functioning CSC has not yet been established. We hypothesized that YAP1, a transcriptional coactivator, and SOX2, a master transcription factor of SCC, may cooperatively induce stemness through transcriptional reprogramming.

Methods We immunohistochemically examined the expression of SOX2 and YAP1 in the CD44 variant 9 (CD44v9)-positive invasion front. A CSC-inducible module was identified through a combination of siRNAs and sphere formation assays. YAP1 and SOX2 interactions were analyzed in vitro.

Results The triple overexpression of SOX2, YAP1, and CD44v9 was significantly associated with poor prognosis. TCGA data revealed that the CSC-inducible module, which was related to EMT and angiogenesis, was significantly correlated with poor prognosis. The KLF7 expression, representatively chosen from the module, also correlated with poor prognosis and was essential for sphere formation and CSC propagation. Sphere stress-activated YAP1 enhanced SOX2 activity.

Conclusions The stress-triggered activation of YAP1/SOX2 transcriptionally reprograms HNSCC for the acquisition of stemness. Triple SOX2, YAP1, and CD44v9 immunostaining assays may be useful for the selection of high-risk patients with functioning CSCs, and YAP1 targeting may lead to the development of a CSC-targeting therapy.

Keywords YAP1 · SOX2 · KLF7 · Cancer stem cell · Head and neck squamous cell carcinoma

Abbreviations

YAP1	Yes-associated protein 1
SOX2	SRY (sex determining region Y)-box 2
KLF	Krüppel-like family of transcription factor
OCT	Octamer-binding Transcription Factor
MMP	Matrix metalloproteinase
SLCO2A1	Solute carrier organic anion transporter family, member 2A1
SERPINB2	Serpin family B member 2
LEMD1	LEM domain-containing 1
DDX60	DExD/H-box helicase 60
BRD4	Bromodomain containing 4
TEAD	TEA domain transcription factor
FOXM1	Forkhead box M1
CYR61	Cysteine-rich angiogenic inducer 61
CTGF	Connective Tissue Growth Factor

Electronic supplementary material The online version of this article (https://doi.org/10.1007/s00432-019-02995-z) contains supplementary material, which is available to authorized users.

✉ Muneyuki Masuda
mmuneyuki@icloud.com

[1] Department of Head and Neck Surgery, National Hospital Organization Kyushu Cancer Center, 3-1-1 Notame, Minamiku, Fukuoka, Fukuoka 811-1395, Japan

[2] Department of Otorhinolaryngology, Graduate School of Medical Sciences, Kyushu University, 3-1-1 Maidashi, Higashiku, Fukuoka, Fukuoka 812-8582, Japan

[3] Department of Pathology, National Kyushu Cancer Center, 3-1-1 Notame, Minamiku, Fukuoka, Fukuoka 811-1395, Japan

Introduction

Head and neck squamous cell carcinoma (HNSCC) is the sixth most common cancer in the world, and approximately half of the patients diagnosed with this disease do

not survive (Leemans et al. 2018). In addition to poor survival rates, the quality of life of patients has not significantly improved in the past decade (Masuda et al. 2016). To solve this issue, research has increasingly focused on the development of novel treatment strategies based on the cell biology of HNSCC. However, in this era of precision medicine, a clinically effective molecular target in HNSCC is not yet to be identified (Morris et al. 2017; Zehir et al. 2017). This is mainly due to the lack of predominant gain-of-function mutations in oncogenes in HNSCC, as was confirmed by The Cancer Genome Atlas (TCGA) Consortium (Cancer Genome Atlas 2015). In view of this distinctive genetic landscape, taken together with the recent remarkable discovery that epigenetic reprogramming also plays fundamental roles in the development and progression of cancer (Feinberg et al. 2016; Zanconato et al. 2018), we postulated that HNSCC is a complex adaptive system that evolves under selective pressures, exploiting the intrinsic epigenetic reprogramming system, thereby developing an ecological tumor microenvironment system, which facilitates the survival and migration of cancer cells (Masuda et al. 2013, 2016). In this process, the acquisition of stemness, i.e., self-renewal and pluripotency, appears to play a central role, responsible for the aggressive phenotypes of cancer, such as resistance to conventional therapy and distant metastasis, which are major determinants of patient prognosis (Shibue and Weinberg 2017). Notably, growing evidence indicates that the cellular transition to this undifferentiated state is highly dependent on epigenetic reprogramming (Shibue and Weinberg 2017; Suva et al. 2013).

In the cells of squamous cell lineages, including the skin and upper aero-digestive epithelium, SOX2 functions as a master transcription factor (MTF) and transcriptionally regulates the self-renewal ability as well as the commitment to the squamous cell lineage in normal progenitor/stem cells (Jiang et al. 2018; Watanabe et al. 2014). As expected, the constitutive activation of this MTF leads to the formation of SCC and is required for the development and maintenance of cancer stem cells (CSC) (Boumahdi et al. 2014; Keysar et al. 2017; Lee et al. 2014). Therefore, it is associated with an unfavorable prognosis of HNSCC (Dong et al. 2014). However, in HNSCC, the precise mechanism for SOX2 activation is not yet to be elucidated. Recently, the oncogenic roles of YAP1 protein have been discussed intensively, including in HNSCC (Segrelles et al. 2018; Totaro et al. 2018; Zanconato et al. 2016). YAP1 is a transcriptional coactivator and was identified as a downstream effector protein of the Hippo pathway, which phosphorylates YAP1 and then retains the inactivated form of YAP1 in the cytoplasm (Totaro et al. 2018). In organogenesis, the Hippo-YAP1 axis is a major regulator of organ size. Under the conditions of normal cell physiology, YAP1 functions as a sensor of the cellular microenvironment, and upon cellular stress, including chronic inflammation, mechanotransduction, and tissue injuries, YAP1 is activated and then emits a regenerative cue in the progenitor/stem cells of the basal layer (Elbediwy et al. 2016). Reflecting this regenerative potential, the organ-specific forced activation of YAP1 protein in genetically engineered mice resulted in tumor formation in the liver, ovaries, and prostate (Zanconato et al. 2016). In HNSCC, YAP1 activation correlates with proliferative regenerative phenotypes as well as poor prognosis (Eun et al. 2017; Garcia-Escudero et al. 2018; Ge et al. 2011; Hiemer et al. 2015; Saladi et al. 2017). It is worth noting that YAP1 can promote induced pluripotent (iPS) cell reprogramming, in combination with SOX2, OCT4, and KLF4 (Lian et al. 2010).

Collectively, we hypothesized that in HNSCC, the stress-triggered activation of YAP1 may collaborate with SOX2 and contribute to the acquisition of stemness through transcriptional reprogramming. In the present study, the nuclear co-expression of YAP1 and SOX2 was prominent in the CSC-enriched invasion front in the oral squamous cell carcinoma (OSCC) samples. We identified a set of candidate gene modules, which may be responsible for the induction of stemness (CSC-inducible module) in the HNSCC cell line and confirmed its clinical significance and CSC-inducing function. In our final assays, we found that the microenvironmental stress-activated YAP1 and the subsequent SOX2 activation were possible mechanisms of action in the transcriptional reprogramming for stemness.

Materials and methods

Clinical samples and staining

We selected 84 formalin-fixed paraffin-embedded surgical specimens obtained from patients with OSCC treated at the National Hospital Organization Kyushu Cancer Center in Japan from 2008 to 2013. All patients received surgical resection as a first line of therapy and their medical charts were reviewed. IHC staining was performed on 4-μm thick slices using anti-YAP1 Ab (Sigma-Aldrich), anti-SOX2 Ab (Cell Signaling), and CD44v9 (kindly provided by Prof. Saya, Keio University) (Aso et al. 2015). All slides were counter stained with Mayer's hematoxylin (Sigma-Aldrich).

Definition of grades and clinicopathological features of YAP1, SOX2, and CD44v9 activation

"YAP1 Activity Grade" was defined by multiplying the "YAP1 Frequency Score" by the "YAP1 Intensity Score", as previously described (Nishio et al. 2016). A score of >7 was classified into the YAP1-high group. "SOX2 Activity Grade" was defined by the "SOX2 Frequency Score", as previously described (Lengerke et al. 2011). A score of >1

was classified into the SOX2-high group. "CD44v9 Score" was defined by the sum of the "CD44v9 Frequency Score" and the "CD44v9 Intensity Score", as previously described (Aso et al. 2015). A score of >1 was considered to be CD44v9-positive. Scoring was performed by two independent observers (K.T. and T.N.) who were blind to the clinical information.

To compare the interactions between YAP1, SOX2, and CD44v9 expression, both Fisher's exact test and Student's *t* test were used to analyze the statistical differences. To compare the overall survival and relapse-free survival rates between two groups of patients (YAP1-high, SOX2-high, CD44v9-positive: triple-positive vs non-triple-positive), Kaplan–Meier curves were generated and a Wilcoxon test was used to analyze statistical differences. The overall survival rate was calculated based on the length of time between the date of surgery and the date of death. The duration of the follow-up was 69.5 months on average (range 3–128 months).

To investigate the factors influencing YAP1/SOX2/CD44v9 activity, the following clinicopathological factors were included in the univariate analyses: age, sex, history of smoking, history of alcohol, T stage (which describes the primary tumor size and site), N stage (which describes the degree of regional lymph node involvement), clinical stage, recurrence, and degree of tumor differentiation (see Supplemental Table 1). Univariate analyses were performed using the Fisher's exact test.

Cell lines and culture

Human HNSCC cell lines HSC3, HSC4 (from JCRB), SCC4, SCC9, Cal27 (from ATCC), and Cal33 (kindly provided by Prof. Silvio Gutkind, University of California) were cultured in EMEM, DMEM, or DMEM/Ham's F12 supplemented with 10% heat-inactivated FBS and 1% penicillin–streptomycin at 37 °C in a 5% CO_2/95% air incubator. The SCC4 and SCC9 culture media were supplemented with 400 ng/ml hydrocortisone in line with a standard protocol.

siRNA transfection and immunoblotting

siRNA targeting of YAP1, SOX2, or KLF7 expression was performed using the siRNA oligonucleotides as follows: siYAP1#1; GGUGAUACUAUCAACCAAA, siYAP1#2; AGAUACUUCUUAAAUCACA, siSOX2#1; ACCAGC GCAUGGACAGUU, siSOX2#2; CAGUAUUUAUCG AGAUAAA, siKLF7#1; GCAUGUCCCGAAAACAAG A, siKLF7#2; GGUUCACCGCUGUCAGUUU. All siRNAs were Silencer Select Pre-designed siRNA (from Ambion). Transfection of siRNA oligonucleotides (10 nM) into HSC4 was performed using Lipofectamine RNAiMAX (Invitrogen) according to the manufacturer's protocol. At 96 h post-transfection, the protein lysates were subjected to immunoblotting. Immunoblotting was carried out using a standard protocol and primary antibodies (Abs) recognizing YAP1 and SOX2 (Cell Signaling). The primary antibodies were visualized using HRP-conjugated. GADPH (Santa Cruz Biotechnology) was uemployed as internal control. The quantification of signal intensity was performed using the Fujifilm Multi Gauge software.

Microarray analysis

The total RNA was isolated from cells using an RNeasy Mini Kit (Qiagen) according to the manufacturer's instructions. RNA samples were quantified using an ND-1000 spectrophotometer (NanoDrop Technologies), and the quality was confirmed using a 2200 TapeStation (Agilent technologies). The cRNA was amplified, labeled with total RNA using GeneChip® WT Pico Kit, and hybridized to Thermo Fisher Scientific Clariom™ D Assay, Human according to the manufacturer's instructions. All hybridized microarrays were scanned using an Affymetrix scanner. The relative hybridization intensities and background hybridization values were calculated using Affymetrix Expression Console™. The raw signal intensities of all samples were normalized using a quantile algorithm with the Affymetrix® Power Tool version 1.15.0 software. To identify up- or downregulated genes, we calculated ratios (non-log scaled fold-change) from the normalized signal intensities of each probe for comparison between the control and experimental samples. Then, we established criteria for the gene regulation: (upregulated genes) ratio ≥ 1.5-fold and (downregulated genes) ratio ≤ 0.66-fold, as previously described (Miyahara et al. 2014). To identify the significantly over-represented GO categories and significant enrichment of pathways, we used the tools and data provided by the Database for Annotation, Visualization and Integrated Discovery (DAVID) (http://david.abcc.ncifcrf.gov/home.jsp) (da Huang et al. 2009a, b). The results were generated from the selected genes downregulated by siYAP1/siSOX2 and upregulated by spheroid cultures as described above.

TCGA data analysis and expression module analysis

We obtained the RNA-seq data and clinical data of 520 HNSCC patients in The Cancer Genome Atlas (TCGA) from the Broad Institute's Firehose (http://gdac.broadinstitute.org/runs/stddata__2016_01_28/data/HNSC/20160128/). We integrated the RNA-seq data along with the clinical data using R version 3.4.2 (The R Foundation for Statistical Computing) and R studio version 1.1.383. The stemness-associated expression module activity was calculated for each case using the average of the expression levels of seven genes (i.e., *MMP1*, *MMP10*, *SLCO2A1*, *SERPINB2*, *LEMD1*,

KLF7, and *DDX60*), as previously described (Hirata et al. 2016). Gene set enrichment analysis (GSEA) was performed using GSEA MSigDB v5.0 (Broad Institute, http://www.broadinstitute.org/gsea/msigdb/index.jsp), as previously described (Subramanian et al. 2005).

Quantitative RT-PCR

Total RNA was isolated as described above. Total RNA (1 µg) was reverse-transcribed using the QuantiTect Reverse Transcription Kit (QIAGEN). The results were quantitated using the $\Delta\Delta C_t$ method. GAPDH was used as the internal control. Fold changes were calculated using the SYBR Green real-time PCR method and the Applied Bio Systems 7700 Sequence Detection System. The primers and probes used for RT-PCR were as follows: KLF7 Forward; 5′-CTCACG AGGCACTACAGGAAAC-3′, KLF7 Reverse; 5′-TGGCAA CTCTGGCCTTTCGGTT-3′, GAPDH Forward; 5′-GTG AAGGTCGGAGTCAACG-3′, GAPDH Reverse; 5′-TGA GGTCAATGAAGGGGTC-3′.

Sphere formation assay

For the sphere-forming assays, 3×10^4 HSC4 cells were seeded in 35 mm µ-Dish (ibidi) with siRNAs. After 1 week, the number of spheroids was counted using a stereoscopic microscope (ZEISS).

Flow cytometry assay

Immunostaining of HSC4 cells with siRNAs was performed by incubating cells with anti-CD44 APC (TONBO Biosciences) antibodies for 15 min prior to FACS analyses. CD44-stained cells were measured using a FACS Calibur instrument.

YAP1 nuclear localization analysis

To visualize the nuclear YAP1 localization of the spheroid cells, the cells were incubated with primary anti-YAP1 Ab (Sigma-Aldrich) followed by incubation with secondary anti-mouse IgG conjugated to Alexa Fluor 568 (Molecular Probes). DAPI (Dojindo) stainings were used for the detection of nuclei. Cells were examined using a DM5000B microscope (Leica).

Motif analysis

We obtained 44 super enhancer regions associated with human KLF7 calculated from H3 K27ac ChIP-seq data of human cell lines and tissues using dbSUPER database (https://asntech.org/dbsuper/). We investigated whether the SOX2-binding motif CTTTGTC is included in these regions and visualized the results using the UCSC genome browser.

Statistical analysis

Unless otherwise stated, all results represent the mean ± standard error of the mean (SEM). The statistical comparison of different two groups was performed using the two-tailed Student's *t* test or Fisher's exact test. The statistical comparison of different multi-groups was performed using the Dunnett's test, or adjusted *p* values using pairwise *t* test with Bonferroni post-test. Differences of $p < 0.05$ were considered statistically significant. For GSEA analysis, Benjamini–Hochberg method was used for statistical analysis, and FDR-*q* value < 0.25 was considered statistically significant. All experiments were repeated at least three times (technical replicates). All statistical analyses were conducted using the JMP Statistical Discovery Software (Version 14.0; SAS Inc.).

Results

YAP1 and SOX2 nuclear co-expression overlaps in CD44v9-positive cells in the invasion front

In our initial study, 84 cases of human oral squamous cell carcinoma (OSCC) (Supplemental Table 1) were immunostained with YAP and SOX2, as well as CD44v9 (Fig. 1a; Supplemental Fig. 1), the marker of CSC in OSCC, as confirmed by previous studies (Aso et al. 2015; Yoshikawa et al. 2013). We then examined the nuclear expression levels of the YAP1 and SOX2 proteins in the same CD44v9-positive regions in the invasion front, where a dense presence of highly de-differentiated cells (CSC and EMT cells) was expected (Aso et al. 2015; Shibue and Weinberg 2017). Interestingly, both YAP1 and SOX2 demonstrated significantly higher expression in the CD44v9-positive invasion front (Fig. 1b), and there was a strong correlation between the expression levels of these two proteins (Fig. 1c). Furthermore, the depth of invasion was significantly advanced in the triple co-high-expression of YAP1, SOX2, and CD44v9 (triple-positive) compared to others (non-triple-positive) (Fig. 1d). Triple-positive group was also more prominent in the older population ($p < 0.001$) and patients who developed recurrences after surgery ($p < 0.001$) (Supplemental Table 1). We then evaluated the prognostic value of this triple co-expression using Kaplan–Meier curves and found that this was significantly associated with a poor overall ($p = 0.0385$) and relapse-free ($p < 0.001$) survival of OSCC (Fig. 1e; Supplemental Table 2). These results suggest that the nuclear co-expression of YAP1 and SOX2 occurs in the

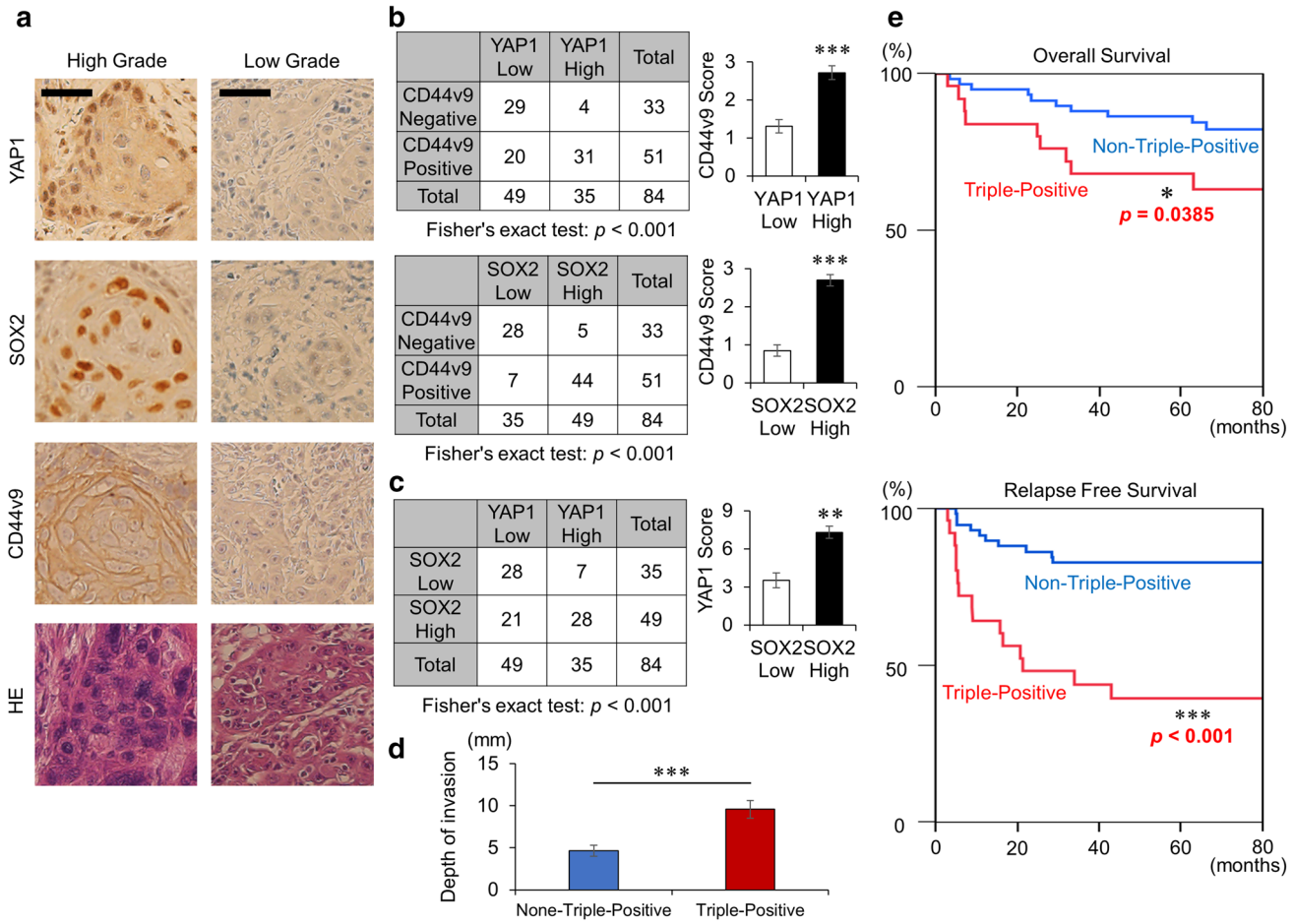

Fig. 1 YAP1 and SOX2 nuclear co-expression overlaps in CD44v9-positive cells in the invasion front. **a** Representative images of YAP1, SOX2, and CD44v9 immunostaining in human OSCCs samples. Scale bar: 25 µm. **b** Correlation between YAP1 or SOX2 and CD44v9 expression. ***$p<0.001$, Fisher's exact test. **c** Correlation between YAP1 and SOX2 expression. **$p<0.01$, Fisher's exact test. **d** Correlation between depth of SCC invasion and triple co-high-expression of YAP1, SOX2, and CD44v9 (triple-positive). ***$p<0.001$, Fisher's exact test. **e** Kaplan–Meier overall (left) and relapse-free survival (right) curves demonstrating the outcomes of 84 tongue cancer patients who underwent surgical resection. The patients were divided into a triple-positive (YAP1-high, SOX2-high, and CD44v9-positive) group ($n=27$) and non-triple-positive group ($n=57$) (see Supplemental Table 1). *$p<0.05$, ***$p<0.001$, Generalized Wilcoxon test

OSCC clinical samples and may collaboratively promote CSC propagation.

Identification of YAP1 and SOX2 common targets genes

In view of this positive result, which supports our hypothesis, we conducted an in vitro study to identify the common target genes of YAP1 and SOX2, both of which are required for the induction of CSC. For this study, we selected an OSCC cell line, HSC4, which demonstrated relatively high YAP1 protein activity measured by the YAP/pYAP ratio as previously described (Hiemer et al. 2015), as well as high SOX2 protein expression (Fig. 2a). Then, the HSC4 cells were either cultured via a sphere formation assay protocol, which is the gold standard for the enhancement of CSC populations in vitro (Bahmad et al. 2018), or were transfected with either siYAP1 or siSOX2 (Fig. 2b). The control cells (normal culture cells or si-scramble transfected cells) and treated cells of each experiment were harvested, and the mRNA levels were compared using a microarray platform. As a result, 1885 genes were found to be downregulated by siYAP1 and 1777 genes by siSOX2, while 4274 genes were found to be upregulated by the sphere formation assays. Among these, 80 overlapped genes were identified as the candidate genes of interest (Fig. 2c).

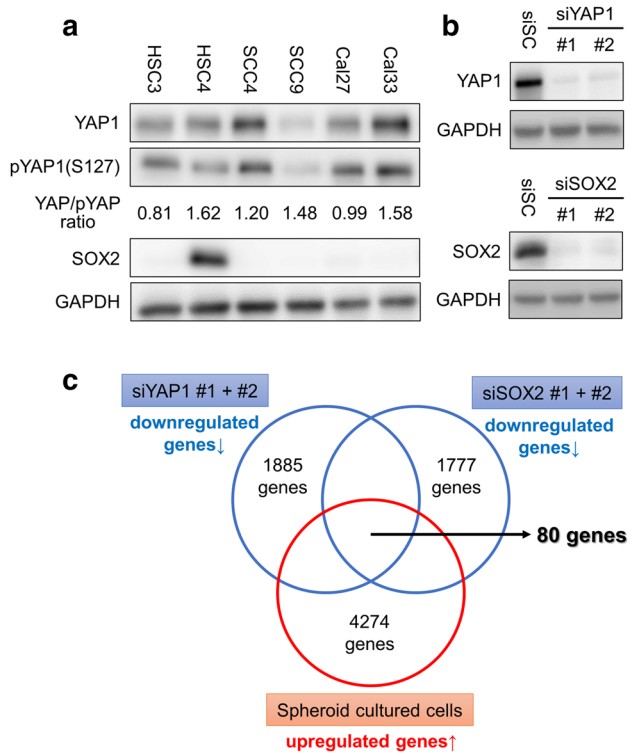

Fig. 2 Identification of YAP1 and SOX2 common target genes. **a** Immunoblots for the detection of YAP1, phospho-YAP1(S127), SOX2, and GAPDH in the indicated HNSCC cell lines. The ratio of YAP1/pYAP1 signal intensity for each sample was determined by densitometry. GAPDH, loading control. **b** Immunoblotting determination of knockdown efficiency of the indicated siRNAs targeting YAP1 or SOX2 in HSC4 cells. GAPDH, loading control. Cells were analyzed at 4 days post-transfection. **c** Venn diagram of extracted genes by microarray analysis. See "Materials and methods" for details

Functional and clinical significances of YAP1 and SOX2 common targets genes

To verify that these candidate genes play a role in the induction of stemness, a gene ontology assay was carried out using the DAVID platform. An enrichment of the genes related to cell motility and crosstalk with the extracellular matrix was observed (Supplemental Table 3), suggesting the phenotypic transition from static epithelial cells to mobile mesenchymal cells. We selected the top 10 upregulated genes (Fig. 3a) in reference to the rank of the sphere formation assays and selected 7 genes (*MMP1, MMP10, SLCO2A1, SERPINB2, LEMD1, KLF7,* and *DDX60*) as the candidate of CSC-inducible modules for further analyses on the basis of the known protein functions and the reported relevance to oncogenesis (Baumeister et al. 2018; Ding et al. 2017; Fu et al. 2016; Harris et al. 2017; Sasahira et al. 2016; Zhu et al. 2015). The clinical significance of this module was analyzed by employing the public TCGA RNA-sequence data obtained from 511 cases of HNSCC. Interestingly, a module high group demonstrated an apparently poor prognosis ($p = 0.0047$) (Fig. 3b) and showed significantly enriched expression patterns related to EMT and angiogenesis (Fig. 3c), reflecting CSC-like traits. Given that SOX2 is a universal MTF of the squamous cell lineage (Jiang et al. 2018; Watanabe et al. 2014), the role of a CSC-inducible module was investigated by employing the TCGA data of lung SCC (LUSCC). Consistent with HNSCC, the module-positive population showed a significantly ($p = 0.0069$) poor prognosis (Fig. 3d), suggesting that this CSC-inducible module may be widely applicable for cancers of squamous cell origin. We then representatively examined the prognostic value of KLF7 expression, a member of the pluripotent KLF family TF (Limame et al. 2014), in the same TCGA HNSCC cohort and found that this was also an adverse prognosis factor ($p = 0.00074$) (Fig. 3e). These results indicate that the YAP1/SOX2-target module (e.g., KLF7) drives tumor progression and is likely to promote the induction of stemness.

YAP1, SOX2, and KLF7 are required for sphere formation

In our next study, we confirmed that YAP1, SOX2, and KLF7 are essential for the sphere-forming capacity of HSC4 cells. The transfection of siKLF7, siYAP1, and siSOX2 significantly inhibited sphere formation (Fig. 4a, b). Interestingly, siKLF7 showed more prominent inhibitory effects on sphere formation compared to siYAP1 and siSOX2. In addition, KLF7 inhibition markedly decreased the CD44-positive CSC population in HSC4 cells (Fig. 4c). These results strongly suggest that KLF7, one of the YAP1/SOX2 common target genes, plays a substantial role in the induction of stemness as an effector molecule in OSCC.

Stress-triggered YAP1 nuclear translocation accounts for SOX2 activation and enhanced KLF7 transcription

Collectively, the data obtained so far suggest that the stress-triggered co-activation of YAP1 and SOX2 cooperatively upregulates the expression of a series of genes and thereby facilitates transcriptional reprogramming for the acquisition of stemness in OSCC. In our final assays, we aimed to elucidate the possible mechanism of this cooperation. Several reports have previously demonstrated mutually upregulating interactions between YAP1 and SOX2 through both direct (e.g., trans-activation) (Bora-Singhal et al. 2015; Lian et al. 2010; Ooki et al. 2018; Seo et al. 2013) and indirect (e.g., through intermediate molecules) (Basu-Roy et al. 2015) interactions. We then examined the effects of silencing of YAP1 on SOX2, and vice versa, using siRNA assays. Unlike previous studies, the downregulation of one gene did not affect the protein expression levels of another gene (Fig. 5a,

a

	Sphere	siYAP1	siSOX2
MMP1	136.481	0.373	0.635
MMP10	78.536	0.537	0.658
SLCO2A1	34.965	0.633	0.651
CLMP	33.440	0.477	0.481
SERPINB2	17.924	0.561	0.578
LEMD1	12.527	0.493	0.432
YPEL2	8.119	0.612	0.419
KLF7	6.878	0.541	0.539
DEFB103A	6.741	0.659	0.443
DDX60	6.246	0.652	0.630

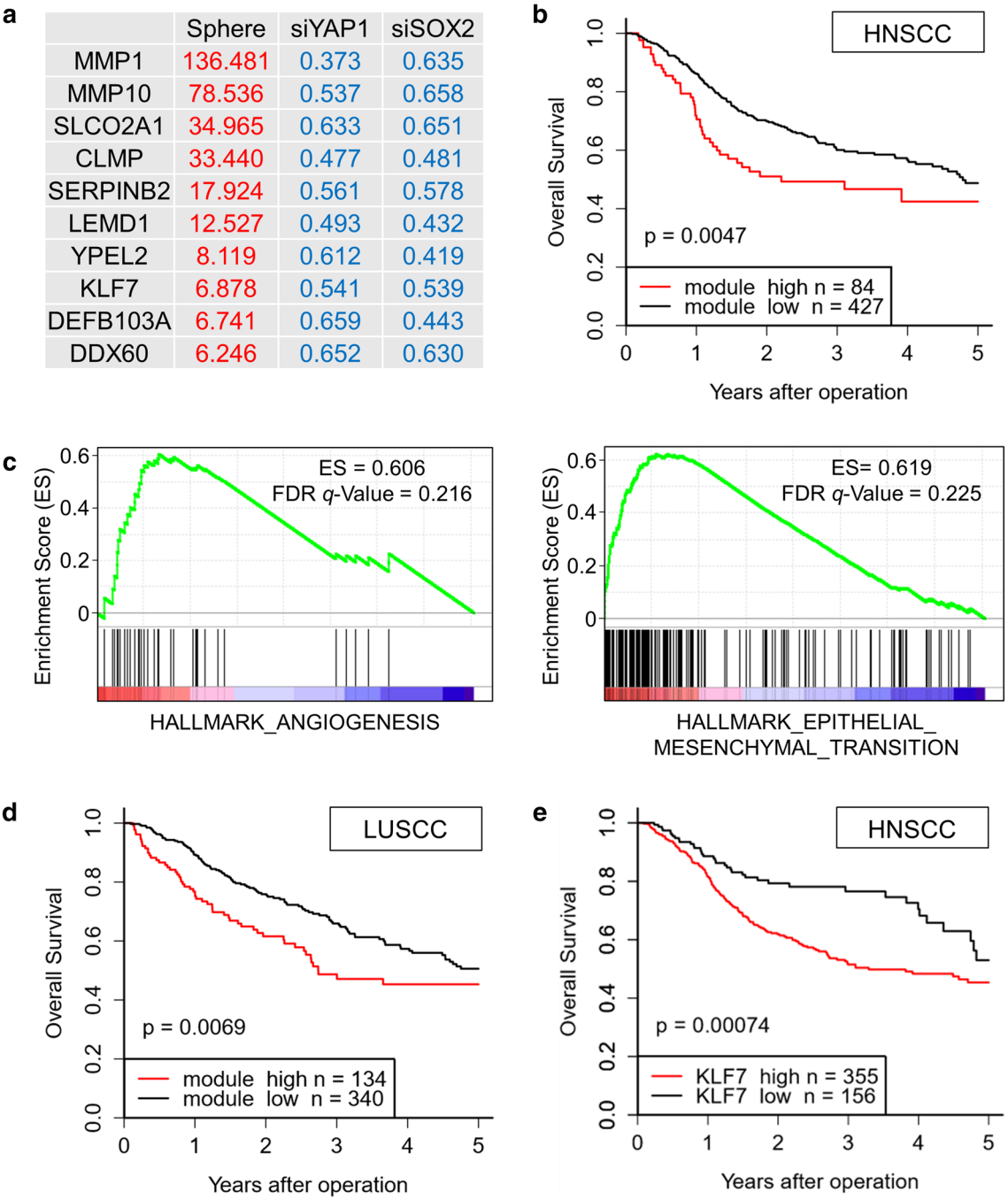

Fig. 3 Functional and clinical significance of YAP1 and SOX2 common target genes. **a** The top ten upregulated genes in reference to the results of the sphere formation and siRNA assays (Fig. 2c) and ranked by the results of sphere formation assays. Sphere indicates spheroid cultured cells and the upregulated relative mRNA ratios of indicated genes are shown. siYAP1 and siSOX2 indicate treatments with the respective siRNAs and the downregulated relative mRNA ratios of indicated gene are shown. **b** Kaplan–Meier overall survival curves on the basis of the module activity (high vs low) determined by the expression of 7 genes (*MMP1*, *MMP10*, *SLCO2A1*, *SERPINB2*, *LEMD1*, *KLF7*, and *DDX60*), employing the TCGA data from HNSCC patients ($n=511$). Module cut off value: 10.1. $^{**}p<0.01$, Generalized Wilcoxon test. **c** Gene set enrichment assay of HALLMARK ANGIOGENESIS and HALLMARK EPITHELIAL MESENCHYMAL TRANSITION gene sets according to the module activity employing the TCGA data from HNSCC patients ($n=511$). FDR $^{*}q$ value <0.25, Benjamini–Hochberg method. **d** Kaplan–Meier curves showing the overall survival on the basis of module activity in the high group vs low group employing TCGA LUSCC patients ($n=474$). Module cut off value: 8.75. $^{**}p<0.01$, Generalized Wilcoxon test. **e** Kaplan–Meier curve showing the overall survival on the basis of KLF7 mRNA high vs low group employing TCGA HNSCC patients ($n=501$). $^{***}p<0.001$, Generalized Wilcoxon test

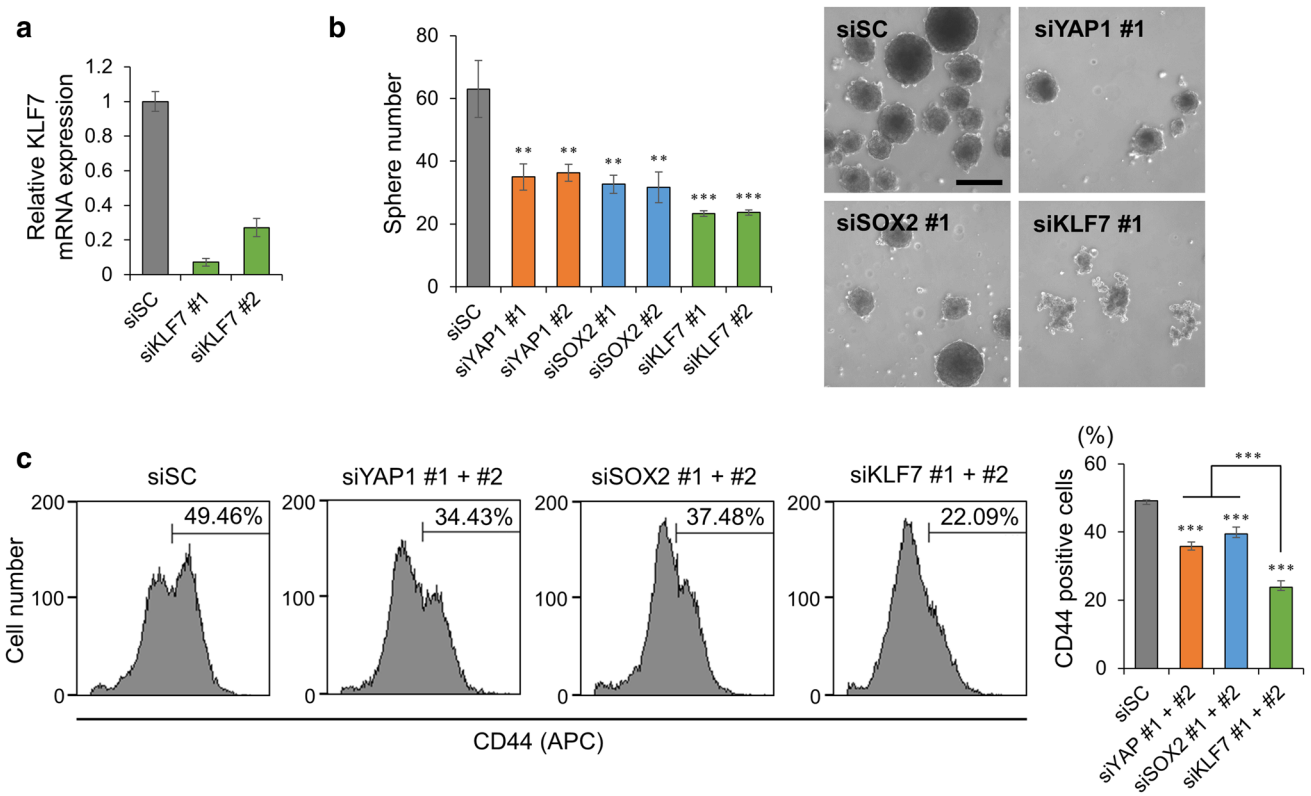

Fig. 4 YAP1, SOX2, and KLF7 are required for sphere formation. **a** Knockdown efficiency of KLF7 by the indicated siRNA targeting measured by RT-qPCR assays in HSC4 cells. Cells were analyzed at 4 days post-transfection. **b** Left panel: sphere number after transfection of indicated siRNAs. Right panel: representative microscopic view of sphere colonies treated with indicated siRNAs. $^{**}p<0.01$, $^{***}p<0.001$, Dunnett's test. **c** Left panel: representative histograms of CD44 (APC)-positive cells treated with indicated siRNAs. Right panel: % of CD44-positive cells. $^{***}p<0.001$, adjusted p values using pairwise t test with Bonferroni post-test

b). This result was also confirmed in the above-mentioned microarray data obtained by siRNA assays and we found that, more interestingly, the sphere culture also did not alter the mRNA expression levels of YAP1 and SOX2 (Supplemental Table 4). Furthermore, in the TCGA data, the mRNA expression levels of YAP1 and SOX2 were mutually exclusive (Fig. 5c). These findings suggest that, at least in HNSCC, YAP1 and SOX2 cooperation occurs independent of the stoichiometric interactions of these proteins. Given that the fundamental function of YAP1 is a transcription coactivator, a possible mechanism of action could be as follows: (1) microenvironmental stress induces the nuclear translocation of YAP1; (2) YAP1 enhances the transcriptional activity of SOX2 and then promotes the expression of target genes. To confirm this theory, we first analyzed the effects of sphere formation stress on the YAP1 protein distribution and found that YAP1 nuclear translocation was markedly enhanced in sphere cells (Fig. 5d). The binding motif search revealed that there is a putative SOX2-binding motif (CTTTGTC) (Mistri et al. 2015) in the regulatory regions of *KLF7* (Fig. 5e). Collectively, these results support our proposed mechanism: stress-triggered YAP1 nuclear translocation activates SOX2 and promotes the transcriptional reprogramming of HNSCC for the acquisition of stemness (Fig. 5f).

Discussion

From a biological standpoint, it is well known that CSC, despite accounting for only a small portion of the tumor, is critical in determining prognosis, including HNSCC (Masuda et al. 2016; Shibue and Weinberg 2017). However, this knowledge has not yet been applied to the clinical setting, mainly due to the lack of reliable methods for the detection of substantially functioning CSC in human tumor samples (Masuda et al. 2016). To address this issue, we evaluated the prognostic significance of two pluripotent factors, YAP1 and SOX2, and the CSC marker of HNSCC, CD44v9, in the identical tumor invasion front, where the enrichment of a functioning CSC population was expected. We found that the triple-positive expression of these proteins was a strong predictor of poor clinical patient outcomes, indicating the presence of functioning CSC in this area. This was further

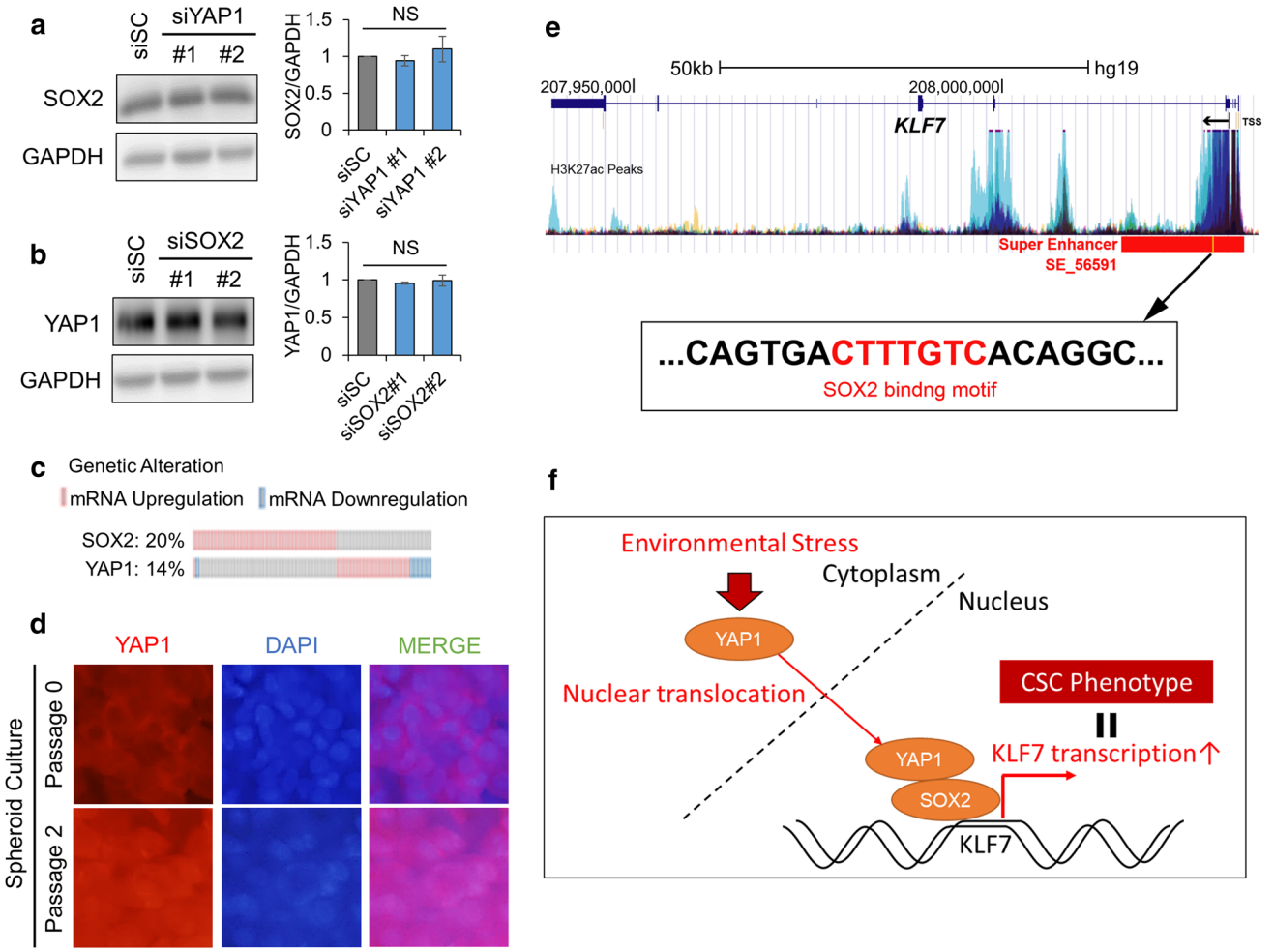

Fig. 5 Stress-triggered YAP1 nuclear translocation and consequent activation of SOX2 and target gene expression. **a** Immunoblots for the detection of SOX2 protein expression in HSC4 cells treated with either control si-scramble siRNA (siSC) or siRNA targeting YAP1. Right panel: quantification of relative SOX2/GAPDH values. *NS* not significant, Dunnett's test. **b** Immunoblots for the detection of YAP1 protein expression in HSC4 cells treated with either control siSC or siRNA targeting SOX2. Right panel: quantification of relative YAP1/GAPDH values. *NS* not significant, Dunnett's test. **c** Interactive comparison of mRNA expression levels of SOX2 or YAP1 examined in the TCGA data of HNSCC patients. **d** Spheroid cultured HSC4 cells with non-passaged and twice passaged cells. Left panels: immunostaining for YAP1 detection (red). Middle panels: immunostaining for DAPI nuclei detection (blue). Right panels: merged images. **e** Screenshot of UCSC genome browser showing H3K27ac occupancy at human KLF7 locus obtained from ChIP-seq data of seven cell lines in ENCODE project. The red bar represents the super enhancer region SE56591 which includes SOX2-binding motif obtained from dbSUPER. TSS, transcription start site. **f** Graphical abstract

supported by in vitro mechanistic studies, which revealed that YAP1 and SOX2 can cooperatively induce CSC traits in HNSCC cells, upregulating a distinctive set of genes related to cellular motility. Moreover, we found that the expression of seven selected genes, a putative CSC-inducible module, was significantly associated with a poor prognosis in the TCGA data. Collectively, it is likely that triple-positive immunostainings for YAP1, SOX2, and CD44v9 in the invasion front could be used as a tool for selecting high-risk patients who are likely to develop CSC-caused tumor recurrences or metastasis after surgical resection. The reliability of this promising finding will have to be investigated further in larger-scale validation studies. To this end, recently developed multiplex IHC platforms, which allow for rapid and automated immunostaining, as well as evaluation with one slide of FFPE sample, may be of great help (Giesen et al. 2014; Tsujikawa et al. 2017).

We identified a putative CSC-inducible module for SCC: *MMP1, MMP10, SLCO2A1, SERPINB2, LEMD1, KLF7,* and *DDX60*. Apart from MMP1 and MMP10, the stemness-inducible role of the other molecule remains to be elucidated. However, recent studies demonstrated that SLCO2A1, a prostaglandin transporter, promoted cellular invasion and inhibited apoptosis through the PI3K/AKT/mTOR pathway in lung cancer (Zhu et al. 2015); SERPINB2, plasminogen activator inhibitor, activated stromal remodeling and local

invasion in pancreatic cancer and breast cancer metastasis (Harris et al. 2017; Jin et al. 2017); LEMD1, a cancer-testis antigen, promoted OSCC invasion (Sasahira et al. 2016); KLF7, a KLF family zinc finger TF, promoted OSCC migration and EMT (Ding et al. 2017); and DDX60, an RNA-helicase, was associated with tumor progression and poor prognosis of OSCC (Fu et al. 2016). In addition, utilizing the TCGA data, we confirmed that the activity of this module was significantly associated with the enrichment of angiogenesis and EMT-related genes, and poor prognosis and KLF7 overexpression was associated with adverse outcomes. These findings support the potential of this module to induce stemness in HNSCC. In view of the marked reduction of the cost and efforts required for RNA-sequencing-based analyses for the surgically resected samples, combinational analyses of the above-mentioned triple-IHC with this CSC-inducible module assay may lead to a more accurate selection of high-risk patients.

The precise function of the transcriptional machinery is becoming increasingly apparent with time (Bradner et al. 2017; Feinberg et al. 2016). In terms of the transcription regulatory elements of targeted genes, the complex composed of transcriptional coactivators, chromatin regulators, TFs, and RNA polymerase II, positively and negatively controls the activity of enhancers and promoters via their activation or inhibition and thereby regulates their transcription. YAP1 is a transcriptional coactivator known to bind to an enhancer activator, p300 (H3k27ac writer); promoter activator, BRD4 (H3k27ac reader and H3K122ac writer); and transcriptional pause release factor, CDK9, and thereby functions as the key hub component of transcriptional regulation (Zanconato et al. 2018). Canonically, the TEAD family of TFs is thought to be the major partner of YAP1. However, several critical TFs, including KLF5, FOXM1, and p53 (gain-of-function mutants) (Di Agostino et al. 2016; Wei et al. 2017; Weiler et al. 2017), are also known to be partner TFs of YAP1. In the present study, we demonstrated that SOX2 may be a novel candidate partner TF of YAP1. Interestingly, in the list of the YAP1/SOX2 common target genes, typical TEAD-targeted genes, including CTGF, CYR61, and BIRC5, were absent (Totaro et al. 2018). This suggests that YAP1 may change partner TFs and target genes cellular context dependently, reflecting the fundamental function of YAP1: a sensor of microenvironmental stresses and a producer of pleiotropic phenotypes (Zanconato et al. 2016). Thus, YAP1 may be a key nexus protein which secures the cellular plasticity and heterogeneity of cancer cells. In addition, a recent striking study demonstrated that when YAP1 binds to BRD4, a super enhancer is formed, which is associated with several cancer types (Zanconato et al. 2018). Here, we found that YAP1/SOX2 may be a critical inducer of stemness in HNSCC; however, the relevance of BRD4 in this process will need to be determined in a future study. Taken together, these findings suggest that YAP1-targeted therapy is a promising method for the treatment of cancers, including in the case of high-risk HNSCC patients. Although a drug that directly targets YAP1 has not yet been discovered, several YAP1 inhibitors exist, including dasatinib, simvastatin, and verteporfin (Nakatani et al. 2017). Furthermore, the effectiveness of small molecule BRD4 inhibitors, such as JQ1, OTX-015, and BAY-1238097, has been confirmed in preclinical studies (Zanconato et al. 2018). YAP1 targeting is within the reach of clinical use and could open up new avenues for the development of CSC-targeting therapy in HNSCC.

Acknowledgements We would like to thank J. S. Gutkind (University of California) for providing the Cal33 cells and Ms. Kimiko Baba for her excellent technical support.

Author contributions Conceptualization: HO, KS, TW, ST, MM; analysis: HO, KS, TN, KT, MM; data curation: HO, KS, TN; writing of the original draft: HO, MM; supervision: TW, ST, TN; project administration: MM; funding acquisition: TW, MM.

Funding We are grateful for the funding provided by the Japanese Society for the Promotion of Science (MEXT/JSPS KAKENHI Grant Number JP16K11255 to M.M., and JP16K11256 to T.W.).

Compliance with ethical standards

Conflict of interest The authors declare that they have no conflict of interest.

Study approval All clinical samples were approved for analysis by the Ethics Committee at National Hospital Organization Kyushu Cancer Center (2015-43).

Informed consent Written informed consent was obtained from all individual participants included in this study.

References

Aso T et al (2015) Induction of CD44 variant 9-expressing cancer stem cells might attenuate the efficacy of chemoradioselection and Worsens the prognosis of patients with advanced head and neck cancer. PLoS One 10:e0116596. https://doi.org/10.1371/journal.pone.0116596

Bahmad HF et al (2018) Sphere-formation assay: three-dimensional in vitro culturing of prostate cancer stem/progenitor sphere-forming cells. Front Oncol 8:347. https://doi.org/10.3389/fonc.2018.00347

Basu-Roy U, Bayin NS, Rattanakorn K, Han E, Placantonakis DG, Mansukhani A, Basilico C (2015) Sox2 antagonizes the Hippo pathway to maintain stemness in cancer cells. Nat Commun 6:6411. https://doi.org/10.1038/ncomms7411

Baumeister P et al (2018) High expression of EpCAM and Sox2 is a positive prognosticator of clinical outcome for head and neck carcinoma. Sci Rep 8:14582. https://doi.org/10.1038/s41598-018-32178-8

Bora-Singhal N, Nguyen J, Schaal C, Perumal D, Singh S, Coppola D, Chellappan S (2015) YAP1 regulates OCT4 activity and SOX2 Expression to facilitate self-renewal and vascular mimicry of

stem-like cells. Stem Cells 33:1705–1718. https://doi.org/10.1002/stem.1993
Boumahdi S et al (2014) SOX2 controls tumour initiation and cancer stem-cell functions in squamous-cell carcinoma. Nature 511:246–250. https://doi.org/10.1038/nature13305
Bradner JE, Hnisz D, Young RA (2017) Transcriptional addiction in cancer. Cell 168:629–643. https://doi.org/10.1016/j.cell.2016.12.013
Cancer Genome Atlas Network (2015) Comprehensive genomic characterization of head and neck squamous cell carcinomas. Nature 517:576–582. https://doi.org/10.1038/nature14129
da Huang W, Sherman BT, Lempicki RA (2009a) Bioinformatics enrichment tools: paths toward the comprehensive functional analysis of large gene lists. Nucleic Acids Res 37:1–13. https://doi.org/10.1093/nar/gkn923
da Huang W, Sherman BT, Lempicki RA (2009b) Systematic and integrative analysis of large gene lists using DAVID bioinformatics resources. Nat Protoc 4:44–57. https://doi.org/10.1038/nprot.2008.211
Di Agostino S et al (2016) YAP enhances the pro-proliferative transcriptional activity of mutant p53 proteins. EMBO Rep 17:188–201. https://doi.org/10.15252/embr.201540488
Ding X, Wang X, Gong Y, Ruan H, Sun Y, Yu Y (2017) KLF7 overexpression in human oral squamous cell carcinoma promotes migration and epithelial–mesenchymal transition. Oncol Lett 13:2281–2289. https://doi.org/10.3892/ol.2017.5734
Dong Z, Liu G, Huang B, Sun J, Wu D (2014) Prognostic significance of SOX2 in head and neck cancer: a meta-analysis. Int J Clin Exp Med 7:5010–5020
Elbediwy A, Vincent-Mistiaen ZI, Thompson BJ (2016) YAP and TAZ in epithelial stem cells: a sensor for cell polarity, mechanical forces and tissue damage. BioEssays 38:644–653. https://doi.org/10.1002/bies.201600037
Eun YG et al (2017) Clinical significance of YAP1 activation in head and neck squamous cell carcinoma. Oncotarget 8:111130–111143. https://doi.org/10.18632/oncotarget.22666
Feinberg AP, Koldobskiy MA, Gondor A (2016) Epigenetic modulators, modifiers and mediators in cancer aetiology and progression. Nat Rev Genet 17:284–299. https://doi.org/10.1038/nrg.2016.13
Fu TY et al (2016) Subsite-specific association of DEAD box RNA helicase DDX60 with the development and prognosis of oral squamous cell carcinoma. Oncotarget 7:85097–85108. https://doi.org/10.18632/oncotarget.13197
Garcia-Escudero R et al (2018) Overexpression of PIK3CA in head and neck squamous cell carcinoma is associated with poor outcome and activation of the YAP pathway. Oral Oncol 79:55–63. https://doi.org/10.1016/j.oraloncology.2018.02.014
Ge L et al (2011) Yes-associated protein expression in head and neck squamous cell carcinoma nodal metastasis. PLoS One 6:e27529. https://doi.org/10.1371/journal.pone.0027529
Giesen C et al (2014) Highly multiplexed imaging of tumor tissues with subcellular resolution by mass cytometry. Nat Methods 11:417–422. https://doi.org/10.1038/nmeth.2869
Harris NLE et al (2017) SerpinB2 regulates stromal remodelling and local invasion in pancreatic cancer. Oncogene 36:4288–4298. https://doi.org/10.1038/onc.2017.63
Hiemer SE et al (2015) A YAP/TAZ-regulated molecular signature is associated with oral squamous cell carcinoma. Mol Cancer Res 13:957–968. https://doi.org/10.1158/1541-7786.MCR-14-0580
Hirata H et al (2016) Decreased expression of fructose-1,6-bisphosphatase associates with glucose metabolism and tumor progression in hepatocellular carcinoma. Cancer Res 76:3265–3276. https://doi.org/10.1158/0008-5472.can-15-2601
Jiang Y et al (2018) Co-activation of super-enhancer-driven CCAT1 by TP63 and SOX2 promotes squamous cancer progression. Nat Commun 9:3619. https://doi.org/10.1038/s41467-018-06081-9
Jin T et al (2017) microRNA-200c/141 upregulates SerpinB2 to promote breast cancer cell metastasis and reduce patient survival. Oncotarget 8:32769–32782. https://doi.org/10.18632/oncotarget.15680
Keysar SB et al (2017) Regulation of head and neck squamous cancer stem cells by PI3K and SOX2J. Natl Cancer Inst 1:1. https://doi.org/10.1093/jnci/djw189
Lee SH et al (2014) SOX2 regulates self-renewal and tumorigenicity of stem-like cells of head and neck squamous cell carcinoma. Br J Cancer 111:2122–2130. https://doi.org/10.1038/bjc.2014.528
Leemans CR, Snijders PJF, Brakenhoff RH (2018) Publisher Correction: The molecular landscape of head and neck cancer. Nat Rev Cancer 18:662. https://doi.org/10.1038/s41568-018-0057-9
Lengerke C et al (2011) Expression of the embryonic stem cell marker SOX2 in early-stage breast carcinoma. BMC Cancer 11:42. https://doi.org/10.1186/1471-2407-11-42
Lian I et al (2010) The role of YAP transcription coactivator in regulating stem cell self-renewal and differentiation. Genes Dev 24:1106–1118. https://doi.org/10.1101/gad.1903310
Limame R, Op de Beeck K, Lardon F, De Wever O, Pauwels P (2014) Kruppel-like factors in cancer progression: three fingers on the steering wheel. Oncotarget 5:29–48. https://doi.org/10.18632/oncotarget.1456
Masuda M, Toh S, Wakasaki T, Suzui M, Joe AK (2013) Somatic evolution of head and neck cancer—biological robustness and latent vulnerability. Mol Oncol 7:14–28. https://doi.org/10.1016/j.molonc.2012.10.009
Masuda M, Wakasaki T, Toh S (2016) Stress-triggered atavistic reprogramming (STAR) addiction: driving force behind head and neck cancer? Am J Cancer Res 6:1149–1166
Mistri TK et al (2015) Selective influence of Sox2 on POU transcription factor binding in embryonic and neural stem cells. EMBO Rep 16:1177–1191. https://doi.org/10.15252/embr.201540467
Miyahara E, Nishikawa T, Takeuchi T, Yasuda K, Okamoto Y, Kawano Y, Horiuchi M (2014) Effect of myeloperoxidase inhibition on gene expression profiles in HL-60 cells exposed to 1,2,4,-benzenetriol. Toxicology 317:50–57. https://doi.org/10.1016/j.tox.2014.01.007
Morris LGT et al (2017) The molecular landscape of recurrent and metastatic head and neck cancers: insights from a precision oncology sequencing platform. JAMA Oncol 3:244–255. https://doi.org/10.1001/jamaoncol.2016.1790
Nakatani K et al (2017) Targeting the Hippo signalling pathway for cancer treatment. J Biochem 161:237–244. https://doi.org/10.1093/jb/mvw074
Nishio M et al (2016) Dysregulated YAP1/TAZ and TGF-beta signaling mediate hepatocarcinogenesis in Mob1a/1b-deficient mice. Proc Natl Acad Sci USA 113:E71–E80. https://doi.org/10.1073/pnas.1517188113
Ooki A et al (2018) YAP1 and COX2 coordinately regulate urothelial cancer stem-like cells. Cancer Res 78:168–181. https://doi.org/10.1158/0008-5472.can-17-0836
Saladi SV et al (2017) ACTL6A is co-amplified with p63 in squamous cell carcinoma to drive YAP activation, regenerative proliferation, and poor prognosis. Cancer Cell 31:35–49. https://doi.org/10.1016/j.ccell.2016.12.001
Sasahira T, Kurihara M, Nakashima C, Kirita T, Kuniyasu H (2016) LEM domain containing 1 promotes oral squamous cell carcinoma invasion and endothelial transmigration. Br J Cancer 115:52–58. https://doi.org/10.1038/bjc.2016.167
Segrelles C, Paramio JM, Lorz C (2018) The transcriptional co-activator YAP: a new player in head and neck cancer. Oral Oncol 86:25–32. https://doi.org/10.1016/j.oraloncology.2018.08.020
Seo E, Basu-Roy U, Gunaratne PH, Coarfa C, Lim DS, Basilico C, Mansukhani A (2013) SOX2 regulates YAP1 to maintain

stemness and determine cell fate in the osteo-adipo lineage. Cell Rep 3:2075–2087. https://doi.org/10.1016/j.celrep.2013.05.029
Shibue T, Weinberg RA (2017) EMT, CSCs, and drug resistance: the mechanistic link and clinical implications. Nat Rev Clin Oncol 14:611–629. https://doi.org/10.1038/nrclinonc.2017.44
Subramanian A et al (2005) Gene set enrichment analysis: a knowledge-based approach for interpreting genome-wide expression profiles. Proc Natl Acad Sci USA 102:15545–15550. https://doi.org/10.1073/pnas.0506580102
Suva ML, Riggi N, Bernstein BE (2013) Epigenetic reprogramming in cancer. Science 339:1567–1570. https://doi.org/10.1126/science.1230184
Totaro A, Panciera T, Piccolo S (2018) YAP/TAZ upstream signals and downstream responses. Nat Cell Biol 20:888–899. https://doi.org/10.1038/s41556-018-0142-z
Tsujikawa T et al (2017) Quantitative multiplex immunohistochemistry reveals myeloid-inflamed tumor-immune complexity associated with poor prognosis. Cell Rep 19:203–217. https://doi.org/10.1016/j.celrep.2017.03.037
Watanabe H et al (2014) SOX2 and p63 colocalize at genetic loci in squamous cell carcinomas. J Clin Investig 124:1636–1645
Wei X, Ye J, Shang Y, Chen H, Liu S, Liu L, Wang R (2017) Ascl2 activation by YAP1/KLF5 ensures the self-renewability of colon cancer progenitor cells. Oncotarget 8:109301–109318. https://doi.org/10.18632/oncotarget.22673
Weiler SME et al (2017) Induction of chromosome instability by activation of yes-associated protein and forkhead box M1 in liver. Cancer Gastroenterol 152:2037–2051, e2022. https://doi.org/10.1053/j.gastro.2017.02.018
Yoshikawa M et al (2013) xCT inhibition depletes CD44v-expressing tumor cells that are resistant to EGFR-targeted therapy in head and neck squamous cell carcinoma. Cancer Res 73:1855–1866. https://doi.org/10.1158/0008-5472.can-12-3609-t
Zanconato F, Cordenonsi M, Piccolo S (2016) YAP/TAZ at the roots of cancer. Cancer Cell 29:783–803. https://doi.org/10.1016/j.ccell.2016.05.005
Zanconato F et al (2018) Transcriptional addiction in cancer cells is mediated by YAP/TAZ through BRD4. Nat Med 24:1599–1610. https://doi.org/10.1038/s41591-018-0158-8
Zehir A et al (2017) Mutational landscape of metastatic cancer revealed from prospective clinical sequencing of 10,000 patients. Nat Med 23:703–713. https://doi.org/10.1038/nm.4333
Zhu Q, Liang X, Dai J, Guan X (2015) Prostaglandin transporter, SLCO2A1, mediates the invasion and apoptosis of lung cancer cells via PI3K/AKT/mTOR pathway. Int J Clin Exp Pathol 8:9175–9181